

Supporting Information

The orientation and electronic structures of multi-layered graphene nanoribbon produced by two-zone chemical vapor deposition

Takahiro Kojima^{1,}, Yang Bao², Chun Zhang^{2,3}, Shuanglong Liu², Hai Xu²,*

Takahiro Nakae¹, Kian Ping Loh^{2,4,} and Hiroshi Sakaguchi^{1,*}*

- ¹ Institute of Advanced Energy, Kyoto University, Uji, 611-0011 Kyoto, Japan
- ² Department of Chemistry, National University of Singapore, 3 Science Drive 3, Singapore, 117543.
- ³ Department of Physics and Graphene Research Centre, National University of Singapore, 2 Science Drive 3, Singapore, 117542.
- ⁴ Centre for Advanced 2D Materials (CA2DM) and Graphene Research Centre, National University of Singapore, 6 Science Drive 2, Singapore 117546.

*e-mail: kojima@iae.kyoto-u.ac.jp, chmlhkp@nus.edu.sg,
sakaguchi@iae.kyoto-u.ac.jp,

Compounds

Synthesis of precursors; a mixture of 3,9- and 3,10-dibromperylene (DBP)¹, and 10,10'-dibromo-9,9'-bianthryl (DBBA)¹ was reported in our previous publications. The other commercially available reagents were used as received, unless otherwise noted.

Au(111) substrates

Au(111) on glass and mica substrates were prepared using an e-beam vacuum-deposition system. Evaporated gold was deposited on the mica or glass substrate, which was heated at 350 °C under a vacuum of 2×10^{-8} Torr. Deposition was performed at a rate of 0.5 \AA s^{-1} , up to 30 nm thickness.

Raman spectroscopy

Raman spectra were recorded using a laser Raman microscope (LV-RAM500/532; Lambda Vision Inc.) with a laser emitting at 532 nm (70 mW). A 0.75/50 \times microscope objective was used. The diameter of the laser spot is considered in the order of 1 μm .

Calculations

Orientation energy calculation

Calculations were carried out using the Materials Studio software suite (BIOVIA Inc.).² The geometries of the 5-AGNR model molecules on Au(111) were optimized using the DTFB+ module with the AuOrg Slater Koster Library. Optimization was performed until the energy converged to less than $0.02 \text{ kcal mol}^{-1}$ and the forces to less than $0.1 \text{ kcal mol}^{-1} \text{ \AA}^{-1}$ at k -point sampling of 0.015 \AA^{-1} ($2 \times 3 \times 2$). All of the Au atoms were fixed for the geometry optimizations. The total Mermin free energies were calculated using the same parameters. The geometries (A) to (F) are defined as (A): 5-AGNR in free space, (B): three layers of Au(111), (C): two pieces of 5-AGNRs with a face-on structure on (B), (D): four pieces of 5-AGNRs with an edge-on structure on (B), (E): two pieces of 5-AGNRs with a face-on structure on (C), and (F); four pieces of 5-AGNRs with an edge-on structure on (C). The orientation energies of the 5-AGNRs were calculated by considering the formation energy per top-most GNR (the total Mermin free energy excluding the top-most GNR subtracted from the total Mermin free energy), the total Mermin free energies, the adsorption energy per top-most GNR (the formation energy of GNRs subtracted from the formation energy per top-most GNR) and the relative stabilities (defined as the differences between (C) and (D), and (E) and (F)). These results are summarized in Table S1.

STM imaging simulation

Calculations were conducted using the Materials Studio software suite (BIOVIA Inc.). Periodic boundary conditions were utilized for simulating the properties of the bulk crystal. The geometries of 7-AGNR was optimized using the DFTB+ module with the CH Slater Koster Library. STM image simulations were performed by single-point energy calculations using the CASTEP² module. GGA-PBE ultrasoft pseudopotentials were chosen.

Band gap calculation

First-principles DFT calculations were performed by utilizing Vienna ab initio simulation package (VASP).^{3,4} The plane-wave cutoff energy was set to 400 eV. The PAW potentials⁵ together with the GGA in the PBE format⁶ were used in all calculations. An energy criterion of 10^{-4} eV was adopted for converging self-consistent field. Structural relaxations were carried out until the Hellmann–Feynman force on each atom is less than $0.02 \text{ eV } \text{\AA}^{-1}$. At least $6 \times 1 \times 1$ k-point sampling in the Brillouin zone were employed in all calculations.

Supplementary Figures

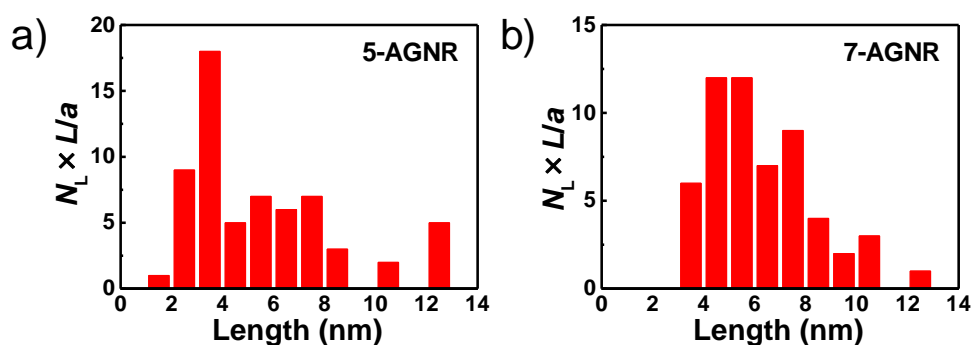


Figure S1 Histogram of chain length distribution of 5-AGNR (a) and 7-AGNR (b) using 1 mg of monomers (based on Figure 1b and c). $N_L \times L / a$, where N_L refers to the counted number of molecular wires having length L (nm) in the STM images, and a corresponds to the monomer-unit length (0.85 nm).

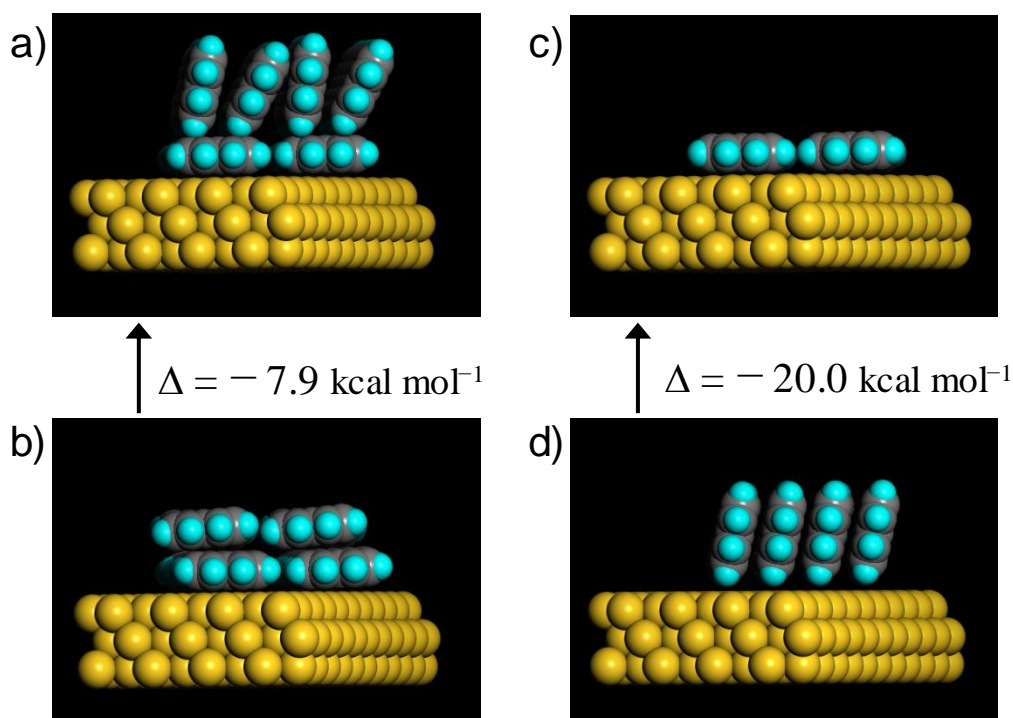
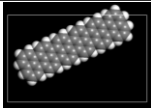
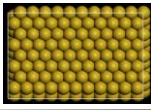
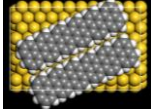
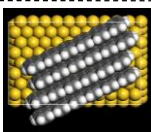
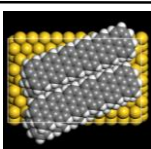
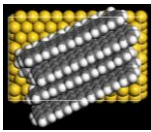


Figure S2. The illustrations of models for DFT calculations of orientation energy. (a) 5-AGNRs with edge-on structures in a top layer lie on GNRs with face-on structures in underlayer. (b) 5-AGNRs with face-on structures in a top layer lie on the underlayer with face-on structures. (c) 5-AGNRs with face-on structures on Au(111). (d) 5-AGNRs with edge-on structures on Au(111).

Table S1 Calculation of orientation energies of 5-AGNR

Geometry	Model system	Optimized geometry	Total Mermin free energy: [Hartree]	Formation energy per a top-most GNR [Hartree]	Adsorption energy per a top-most GNR [Hartree]	Relative stability
A	1 x 5AGNR in free space		-114.0657286	-114.0657286	0	
B	Au(111)		-757.2488038			
C	2 x 5AGNR Face-on Au(111)		-985.4500877	(C-B)/2 -114.1006419	-0.034913	-0.031788 [H] -19.95 kcal/mol
D	4 x 5AGNR Edge-on Au(111)		-1213.5242179	(D-B)/4 -114.0688535	-0.0031249	0
E	2 x 5AGNR Face-on 2 x 5AGNR Face-on Au(111)		-1213.5598436	(E-C)/2 -114.0548779	+0.010851	0
F	4 x 5AGNR Edge on 2 x 5AGNR Face-on Au(111)		-1441.7199541	(F-C)/4 -114.0674666	-0.0017380	-0.012589 [H] -7.899 kcal/mol

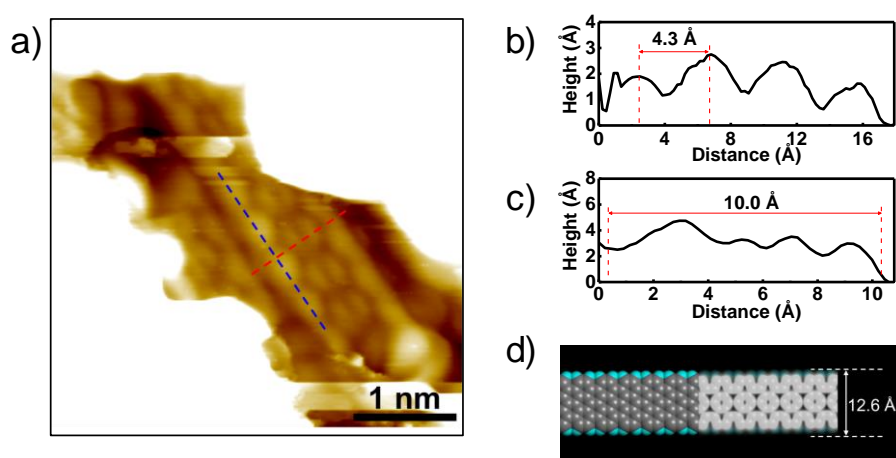


Figure S3. Structural analysis of 7-AGNR in underlayer obtained from 1 mg of DBBA. (a) STM image of 7-AGNR obtained from 1 mg of DBBA ($I_t = 20$ pA, $V_s = -2.0$ V). (b) Cross sectional analysis of the blue dotted line in (a). (c) Cross sectional analysis of the red dotted line in (a). (d) The space filling model of 7-AGNR overlaid on the STM simulation.

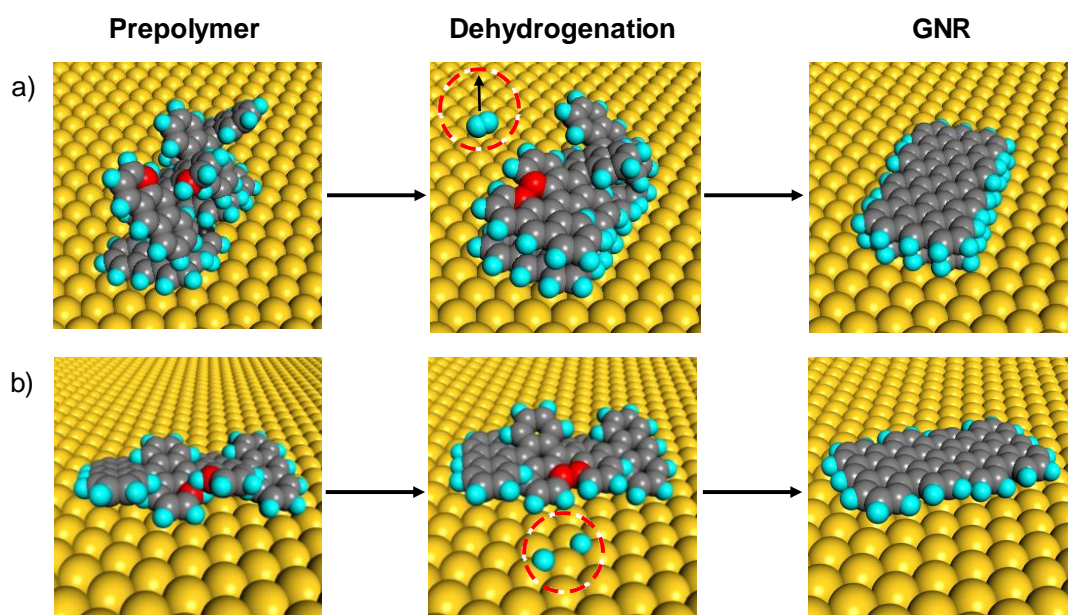


Figure S4. (a) Illustration of proposed dehydrogenation mechanism in multilayer. (b) Previously reported catalytic dehydrogenation mechanism on Au(111).

References

- 1 Sakaguchi, H.; Kawagoe, Y.; Hirano, Y.; Iruka, T.; Yano, M.; Nakae, T. Width-controlled sub-nanometer graphene nanoribbon films synthesized by radical-polymerized chemical vapor deposition. *Adv. Mater.*, **2014**, *26*, 4134-4138.
- 2 Clark, S. J.; Segall, M. D.; Pickard, C. J.; Hasnip, P.J.; Probert, M. J.; Refson, K.; Payne M. C. First principles methods using CASTEP. *Z. Kristallogr.* **2005**, *220*, 567-570.
- 3 Kresse, G.; Hafner, J. Ab initio Molecular-Dynamics for Liquid Metals. *Phys. Rev. B* **1993**, *47*, 558–561.
- 4 Kresse, G.; Furthmüller, J. Efficient Iterative Schemes for Ab Initio Total-Energy Calculations Using a Plane-Wave Basis Set. *Phys. Rev. B* **1996**, *54*, 11169–11186.
- 5 Blöchl, P. E. Projector Augmented-Wave Method. *Phys. Rev. B* **1994**, *50*, 17953–17979.
- 6 Perdew, J. P.; Burke, K.; Ernzerhof, M. Generalized Gradient Approximation Made Simple. *Phys. Rev. Lett.* **1996**, *77*, 3865–3868.